University of Baghdad
College of Engineering
JOURNAL OF ENGINEERING

Journal of Engineering
journal homepage: www.jcoeng.edu.iq
Volume 32 Number 4 April 2026

Assessing the Accuracy of NASA POWER Data in Estimating Weather Variables (Precipitation and Temperature) for Khassa Chai River Watershed

Alaa Jasim Mohammed [1, *], **Basim Sh. Abed** [2], **Maysam Th. Al-Hadidi** [1, 3]

[1]Department Water Resources Engineering, College of Engineering, University of Baghdad, Baghdad, Iraq
[2]Al-Hadi University, Baghdad, Iraq
[3]College of Artificial Intelligence, University of Baghdad, Baghdad, Iraq

ABSTRACT

This study intends to evaluate the accuracy and reliability of satellite data from the NASA POWER project in capturing important climatic variables, which are precipitation and air temperature, compared with data collected from the National Climate Data Center (NCDC) ground-based weather stations located in the Khassa Chai River basin. The basin has a topographic gradient beginning on the northeastern highlands and sloping towards the southwest. The Khassa Chai River Basin experiences a semi-arid climate, with hot, dry summers and relatively cold and wet winters. Daily precipitation and temperature records (2010–2024) were collected from four weather stations, in addition to records from the NASA POWER recording at the nearest grid points. To evaluate the reliability of the datasets from NASA POWER, this study used several relevant statistical indicators (i.e., the coefficient of determination (R^2), correlation coefficient (CC), Nash-Sutcliffe efficiency (NSE), mean bias error (MBE), and root mean square error (RMSE)) at daily, monthly, and yearly time scales. The analysis of precipitation indicated an excellent fit between the NASA POWER satellite data and in-situ data. For monthly comparison, the R^2 was 0.89, and the CC was 0.94, while for annual comparison, the R^2 was 0.81, and the CC was 0.88. Overall, the fit improved with longer time scales, which indicates the ability of the satellite data to accurately capture precipitation trends over time. The range of NSE values from 0.72 to 0.87 also reinforces the ability of the data to reproduce precipitation changes over time.

Keywords: NASA POWER, Khassa Chai river, Satellite climate data validation, Rainfall and temperature analysis, Spatial and temporal distribution.

1. INTRODUCTION

In general, the input data for the models are daily weather records. The quality of weather data is the key to obtaining accurate results, because it may differ greatly from one source

*Corresponding author
Peer review under the responsibility of University of Baghdad.
https://doi.org/10.31026/j.eng.2026.04.07

Article received: 21/11/2025
Article revised: 20/02/2026
Article accepted: 02/03/2026
Article published: 01/04/2026

to another without strict validation and analysis; as a consequence, the uncertainty increases in the outputs **(Ali et al., 2011; Faybishenko et al., 2022; Zheng and Zhang, 2025)**. Daily rainfall and mean daily air temperature are the two most fundamental climatic components affecting hydrological modelling behaviour **(Schreiner et al., 2021; Li et al., 2024; Rasheed et al., 2024; Nama et al., 2024; Abidalla and Abed, 2025)**. However, regional studies have to cope with a scarcity of weather data, which is due to either the spatial gaps in the coverage by ground-based stations **(Barron et al., 2024; Qin et al., 2022)** or even of its absence at all sites **(Wakweya, 2023; Van et al., 2024)** The precision of weather data is very important in influencing the potential application range and trustworthiness of hydrological models **(Singh et al., 2023; Ansari et al., 2023)**, because these data are fundamental to understanding and describing the constituent elements of the hydrological cycle **(Al Thamiry and Azzubaidi, 2020; Yang, 2021)**. Ground-based monitoring stations that record data directly are the most accurate source for measuring climatic variables **(Merlone et al., 2024; Langsdale et al., 2025; Al-Juhaishi et al., 2024)**. However, their limited availability and high costs for construction and maintenance mean they are not found in many parts of the world **(Schuldt et al., 2021; Newman et al., 2023)**.

When data from meteorological stations is missing or coverage is sparse, reanalysis data from global atmospheric models serve as reliable alternatives. These models help provide climate inputs for hydrological models **(Gu et al., 2023; Jiang et al., 2024; Mankin et al., 2025)**. This data comes from numerical assimilation systems that combine satellite observations with surface and marine data. They provide long-term time series that represent the features of the atmosphere and Earth's surface **(Li et al., 2024; Fu et al., 2024; Bai et al., 2025)**. The National Aeronautics and Space Administration (NASA) has also made climate data available through its NASA POWER (Prediction of Worldwide Energy Resources) website, which is connected to the Langley Research Center to supply free global climate data for environmental, hydrological, and renewable energy research **(Hegyi et al., 2023; Quansah et al., 2024)**.

Recently, NASA POWER reanalysis datasets have become easily accessible online with high-resolution climate data available at both local (0.5° × 0.5°) and global (1° × 1°) scales **(Tayyeh and Mohammed, 2023; Kheyruri et al., 2024; Ibrahim and Al-Dabbas, 2021)**. The dataset includes meteorological variables such as near-surface air temperature, relative humidity, precipitation, solar radiation, wind speed, and wind direction **(Rodrigues et al., 2021; Jia et al., 2024)**. NASA data are created with advanced numerical simulations based on weather prediction models while combining ground-based and satellite observations, which improves accuracy and reduces uncertainty **(Saleh et al., 2024; Mutlu, 2025; Ali et al., 2023)**. The NASA POWER website has an interactive interface that allows researchers and users to easily access reliable climate data for hydrology, renewable energy, and environmental studies **(Liu et al., 2020; Budamala and Mahindrakar, 2022)**. The platform provides three types of climate data: single-point, regional endpoint, and global endpoint data, which are derived from a combination of satellite and ground-based weather station observations **(Baumann et al., 2016; Shao and Nerger, 2024)**.

Numerous studies have evaluated the accuracy of various meteorological variables within a variety of reanalysis datasets; however, there is a small number of NP studies that evaluated the validity and accuracy across multiple countries **(Negm et al., 2017; Monteiro et al., 2018; Aboelkhair et al., 2019; Hazra et al., 2019; Al-Kilani et al., 2021; Marzouk, 2021)**. There is a need for studies to assess NASA POWER satellite data analysis within the Khassa Chai River basin.

This gap in research is especially pertinent due to the need for ground-based meteorological data in the Khassa Chai River Basin at three timescales (daily, monthly, and yearly), to compare the quality of climate data products over the river basin over both time and space. The current study examines the temporal and spatial assessment of the NASA POWER precipitation and mean temperature product over 15 years, from 2010 to 2024, at 0.5 resolution, in an effort to close this gap.

2. MATERIALS AND METHOD

2.1 Selected Site

The Khassa Chai River Basin is located in northern Iraq within Kirkuk Governorate, between latitudes 35.0°–35.7° North and longitudes 44.2°–44.7° East with 468 Km^2 area **(Al-Kahachi et al., 2022; Mahmood and Mohammed-Ali, 2025)**, as shown in **Fig. 1**. It is an important sub-basin that drains into the Tigris River. The basin features diverse topography, ranging from the eastern highlands of the Zagros Mountains, which reach about 900 meters above sea level **(Mahmoud and Kasim, 2019)**, to central areas with undulating terrain at 400–600 meters, and flat plains in the west near Kirkuk at roughly 250–300 m.

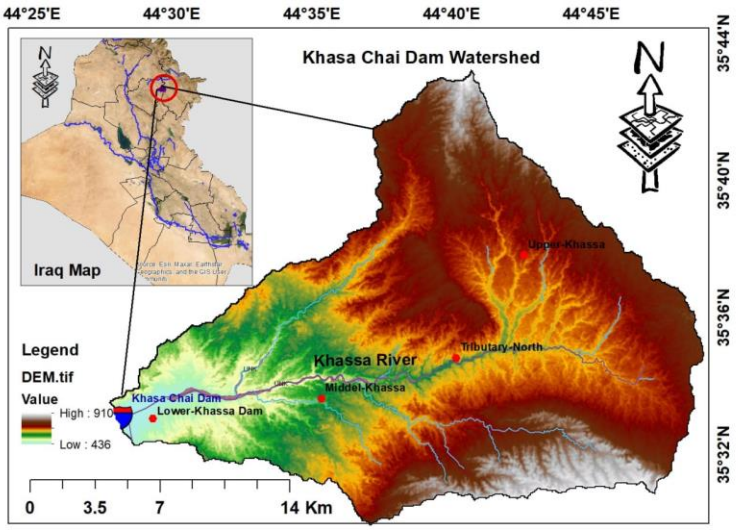

Figure 1. A Map showing the location of the Khassa Chai River basin.

Elevation differences influence surface runoff and rainfall, where higher areas receive more rainfall while depletion of rainfall is towards the plains **(Al-Khafaji et al., 2017; Dawood, 2024)**. Temperature and precipitation, in the semi-arid and Mediterranean climate zone of the study area, have cold and wet winters and hot and dry summers **(Al-Qurnawi, 2014)**. Average annual precipitation may vary between 417 mm, depending on elevation. Summer temperatures can exceed 37 °C **(Mahmood and Mohammed-Ali, 2025)**, and winter temperatures in mountainous terrain may drop below 5 °C. The study area will also experience very high evaporation rates due to long sunny days and long dry seasons, which limit the ability of this precipitation to recharge the local aquifers. Climate change will worsen the regional changes in precipitation and temperature in the basin, creating uncertainty in water resources from intense periods of drought or heavy rain. The Methods and the sample are summarized in **Fig. 2**.

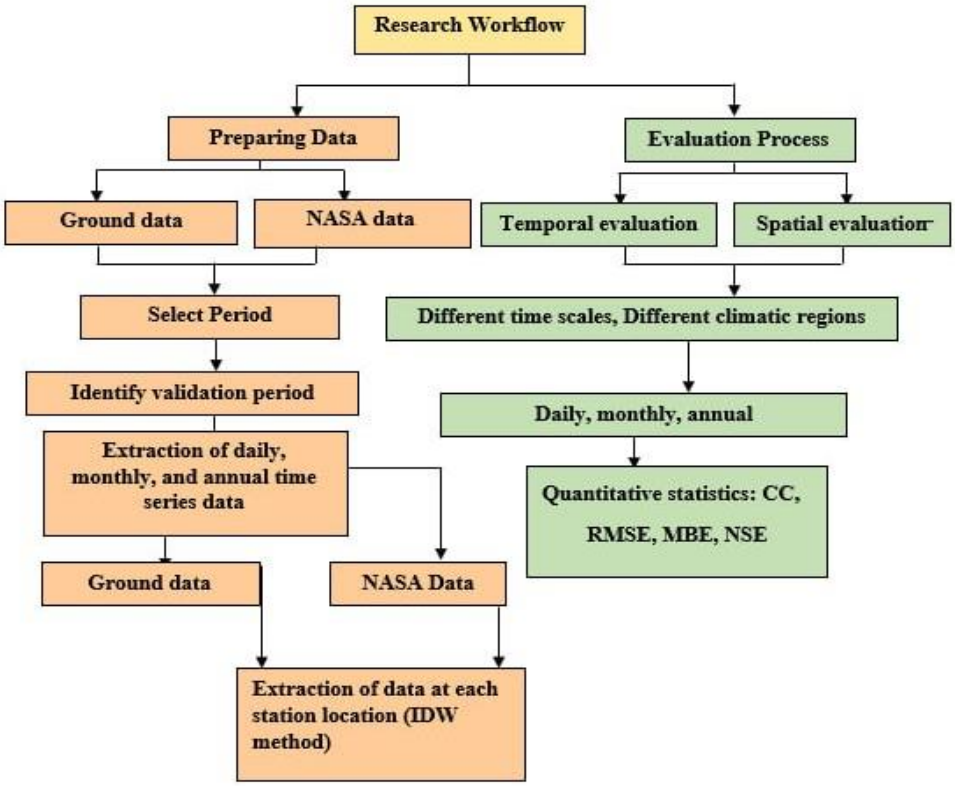

Figure 2. Flow chart adopted for this study.

2.2 Collected Weather Data

The Iraqi government provides daily, monthly, and annual records of weather conditions from four ground-based weather stations distributed across the Khassa River Basin (KRB) from 2010 to 2024, as shown in **Table 1**. However, many of these stations still suffer from data gaps or interruptions, which limit the accuracy of hydrological and climatological studies. To overcome this deficiency, satellite data can be used as an alternative to fill these gaps. The platform provides data for the same meteorological variables recorded by the ground stations, such as precipitation and average air temperature, for the same observation period, extracted at the nearest grid point to the target location. Thus, NASA POWER data enables accurate hydrological and climatological simulations in areas lacking complete ground-based monitoring coverage.

Table 1. Geographic characteristics of weather stations in the KRB.

Station No	Name	Latitude (N)	Longitude (E)	Altitude (m)	Avg Precipitation (mm)	Avg Temperature (^{o}C)
G1	Daquq	35° 10' 8"	44° 25' 49"	640	302.22	21.88
G2	Chamchamal	35° 33' 50	44° 28' 1"	517	258.42	22.17
G3	Kirkuk	35° 42' 25	44° 39' 43"	475	293.825	21.77
G4	Khasa Chai	35° 33' 32	44° 29' 2"	315	290.175	21.75

2.3 Accuracy Evaluation

Among the most important tools for verification in estimating or predicting data compared to physically measured data is statistical analysis **(Bhandari et al., 2012; Valipour, 2016)**.

In this study, an Excel (2021) equation was used to conduct various statistical methods to investigate daily, monthly, and annual NASA POWER data obtained through ground-based data observation. Accuracy is evaluated by several statistical measures, specifically correlation coefficient (CC), root mean square error (RMSE), mean error (ME, coefficient of determination (R^2), and the Nash–Sutcliffe efficiency coefficient (NSE). These statistical measures could be different based on the objective of the study, the nature of the data, and the method of assessing the model's performance. Statistical measurements will typically assess the degree of deviation between the predicted value and the measured value to justify the reliability (or credibility) of the results. Statistical measures used here to assess accuracy are summarized in **Table 2**, and include (N) number of samples, projected value (Pi), and observed value (Oi).

Table 2. Statistical metrics are used to evaluate the accuracy of weather data.

No	Parameter Name	Equation	Range	Unit	Optimal value
1	Coefficient of Determination (R^2)	$R^2=[\frac{\sum_{i=1}^{n}(O_i-O_a)(P_i-P_a)}{[\sum_{i=1}^{n}(O_i-O_a)^2]^{0.5}[\sum_{i=1}^{n}(P_i-P_a)^2]^{0.5}}]^2$	0 - 1	-	1
2	Mean Bias Error (MBE)	$MBE\ (MAE) = \frac{\sum_{i=1}^{n} P_i - O_i}{n}$	0 - +∞	mm	0
3	Sutcliffe Efficiency Coefficient (NSE)	$NES = 1 - \frac{\sum_{i=1}^{n}(O_i - P_i)^2}{\sum_{i=1}^{n}(O_i - O_a)^2}$	0 - 1	-	1
4	Correction Coefficient (CC)	$CC=\frac{\sum_{i=1}^{n}(O_i-O_a)(P_i-P_a)}{[\sum_{i=1}^{n}(O_i-O_a)^2]^{0.5}[\sum_{i=1}^{n}(P_i-P_a)^2]^{0.5}}$	- ∞- +∞	-	1
5	Root Mean Squared Error (RMSE)	$RMSE = \sqrt{\frac{\sum_{i=1}^{N}(p_i-o_i)^2}{N}}$	0 - +∞	mm	0

3. RESULTS AND DISCUSSION

3.1 Spatial Distribution Weather Pattern

In order to calculate annual climatic averages, rainfall and monthly temperature average data available from all meteorological stations in the study area during the period 2010 to 2024 were collected. Subsequently, the values were analyzed using the GIS environment (ArcGIS 10.5) to conduct spatial interpolations for the Inverse Distance Weighting (IDW) method, which estimates the spatial distribution of climatic variables in the location between stations. This analysis enabled the generation of annual climate maps with spatial rainfall and temperature distributions for all sub-basins in the research area. The spatial analysis results that re shown in **Figs. 3 and 4** indicate that the average annual rainfall values ranged from 258 to 310 mm and average annual temperature values ranged from 20.98 to 22.84 °C, and revealed a clear climate gradient associated with upper area topography and elevation differences in the basin. Precipitation amounts decrease progressively from the higher values in the eastern higher zones to the lower values in the western lower zones. The eastern and southeastern part of the basin has the highest precipitation amounts, exceeding 300 mm/year annually, just east of the western slopes of the Zagros Mountains. These higher precipitation amounts are attributed to the higher elevations, causing condensation of the water vapor transported by moist air masses from the Arabian Gulf and the Mediterranean Sea. This leads to higher amounts of orographic precipitation.

The central portion of the basin, where the topography is more undulating, shows moderate precipitation values ranging from 270-290 mm/year, where the influence of the topographic

gradient weakens. In the western and northwestern parts of the basin, just southeast of the city of Kirkuk, precipitation amounts decrease significantly to only 250-270 mm/year. The flatter terrain and farther distance from the direct influence of mountains, in addition to hotter temperatures and increased evaporation, are influencing both the lower trends. In summary, this spatial gradient in precipitation shows the effect of height and topography as primary factors affecting precipitation in the basin, and suggests that recharging of groundwater and surface water is more effective in eastern areas, as opposed to the lower western regions. The spatial distribution of temperature in the Khassa Chai River Basin varies considerably based on the following factors: elevation, topographic slope, and the effects of solar exposure for the year.

In the case of temperature, while the eastern parts of the basin, which have elevations greater than 700-900 m above sea level, have the coldest average annual temperatures between 20.5–21.5 °C due to variation in elevation, nighttime cooling, and localized and regional cold air masses from the Iranian highlands, central areas in the region have intermediate temperature at 21.5–22.2 °C due to the rolling terrain leading to cooler temperatures. In contrast, lower-lying western areas bordering Kirkuk, the lowest average temperatures and greater temperatures of 22.8 °C or higher were observed as a result of reduced elevation and therefore more exposure to the sun's rays, leading to decreased cooling effects and longer periods of sunshine over the summer months. The distribution of solar radiation values is slightly different. Values are highest in the western and south western areas of the region (due in part to low vegetation cover and flat terrain allowing more solar energy to reach the surface). Values of solar radiation are comparatively lower in the eastern mountainous regions because of the cloudy cover, the slope angles, and the topographic shading from the continuous elevations. Overall, the relationship between the two variables is clearly inverse within the basin, in the sense that as elevation increases and direct solar radiation decreases, temperatures become lower, and vice versa in lower elevations. These thermal and radiation characteristics will continue to define micro-climatic variation in the basin and subsequently determine evaporation rates or water balance variables, which directly affect hydrological processes in the river system.

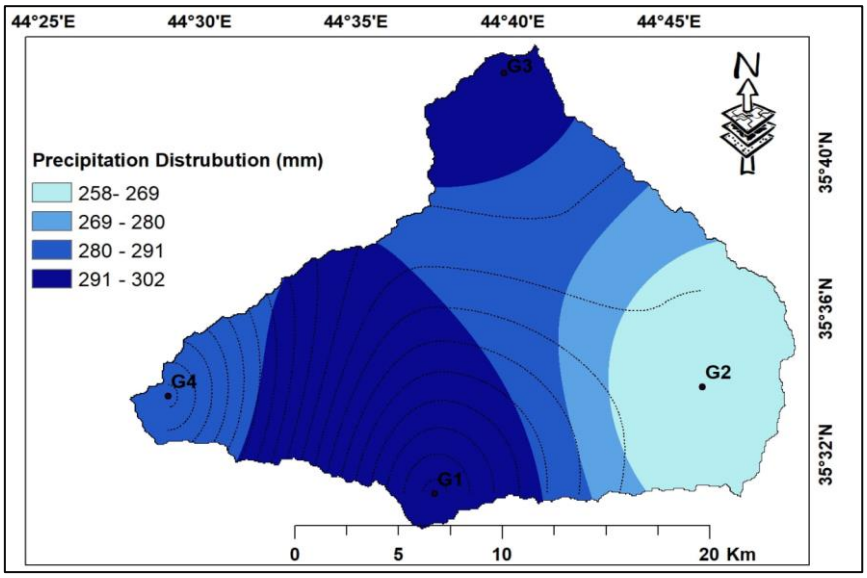

Figure 3. Spatial distribution of average annual precipitation in the Khassa Chai River Basin for the period 2010–2024.

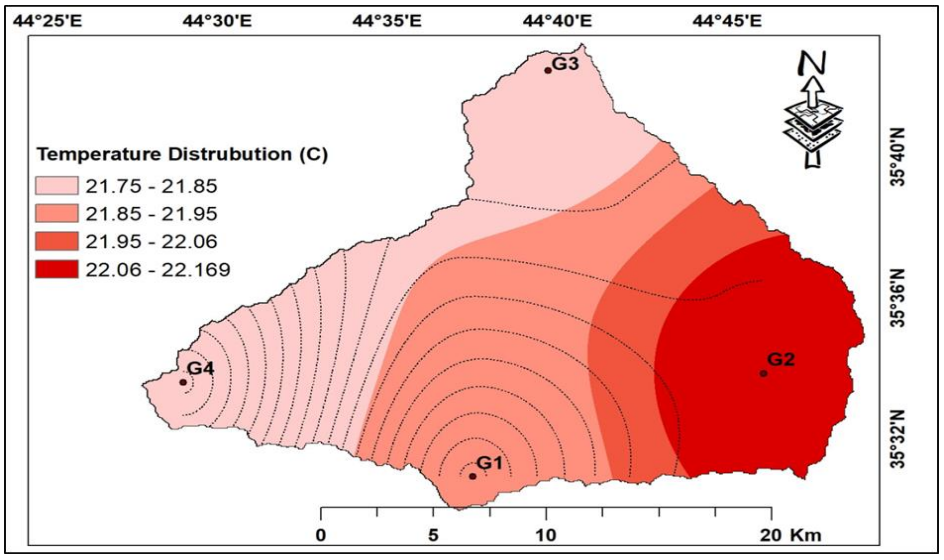

Figure 4. Spatial distribution of average annual temperature in the Khassa Chai River Basin for the period 2010–2024.

3.2 Climate Variables Evaluation

3.2.1 Precipitation

Figs. 5 and 6 show the statistical analysis of the performance evaluation of precipitation data obtained from the NASA POWER platform compared to measured data from ground stations within the Khassa Chai River basin, at three temporal scales: daily, monthly, and annual. A set of statistical indicators (R^2, CC, NSE, RMSE, MBE) was used to assess the level of accuracy and bias in the satellite estimates relative to ground observations. The correlation coefficient (CC) results indicate a good correlation between the NASA POWER data and the field-measured data, with values ranging from 0.75 to 0.79, recording the highest value at station G1 (CC = 0.79) and the lowest at G3 (CC = 0.75). This acceptable correlation reflects the ability of the satellite system to represent daily variations in precipitation despite the intermittent nature of rainfall in the region.

There were similar results for the coefficient of determination (R^2), with daily values between 0.75 and 0.78, which means roughly 75% of the variance in the observed values could be attributed to satellite-derived data. The minor discrepancy at the stations is likely due to the bathymetric nature of the basin impacting the distribution of rainfall in the local areas.

Daily RMSE values showed a notable disparity across stations, with the maximum value of 4.30 mm at G1, and reaching 7.65 mm at G3. RMSE values demonstrated diminished model performance at locations with high spatial variability in precipitation. Daily MBE ranged from 1.45 to 10.32 mm, indicating a slight positive overestimation bias at certain stations, mainly in the central areas of the basin. NSE index showed acceptable daily values as well, indicating NASA POWER data captured the typical daily precipitation trend, while at some locations, positional variability was very limited and of little concern.

Correlation and accuracy metrics improved at the monthly level above 0.85 for most stations, indicating this is an improved correlation between NASA POWER data and observed precipitation. The CC also increased to between 0.87 and 0.89, which supports that the use of temporal aggregation diminishes the effect of short-term fluctuations.

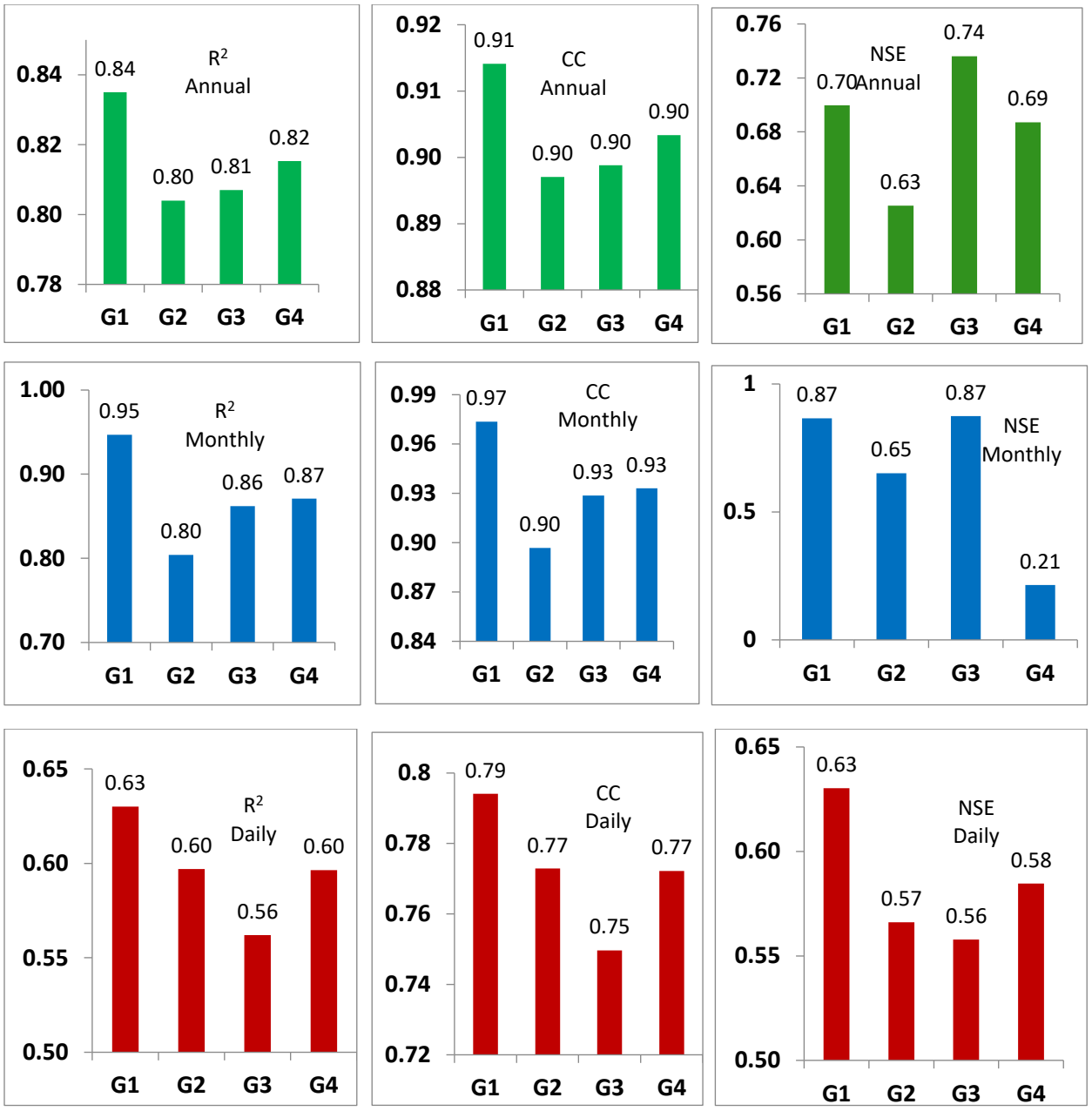

Figure 5. Statistical evaluation (R^2, CC, NSE) of precipitation using NASA POWER data compared to ground measurements at three-time scales (daily, monthly, and annually).

Monthly RMSE values reflected significantly lower values compared to the daily RMSE values, at values between 0.13 and 2.09 mm, reflecting greater accuracy in the monthly measure. Likewise, monthly MBE values were significantly reduced, suggesting that random biases related to daily errors were minimized in the monthly measure. Monthly NSE values were between 0.4 and 0.63, indicating that the satellite model provides accurate and relative estimates in greater agreement with observations at most stations. Annual indicators performed best among all temporal dimensions with R^2 levels approaching 0.81 for most stations, which indicates a high level of agreement with other NASA POWER data and the observed measures. The CC values ranged between 0.77 and 0.79 and further strengthened confidence in the accuracy of the data longitudinally.

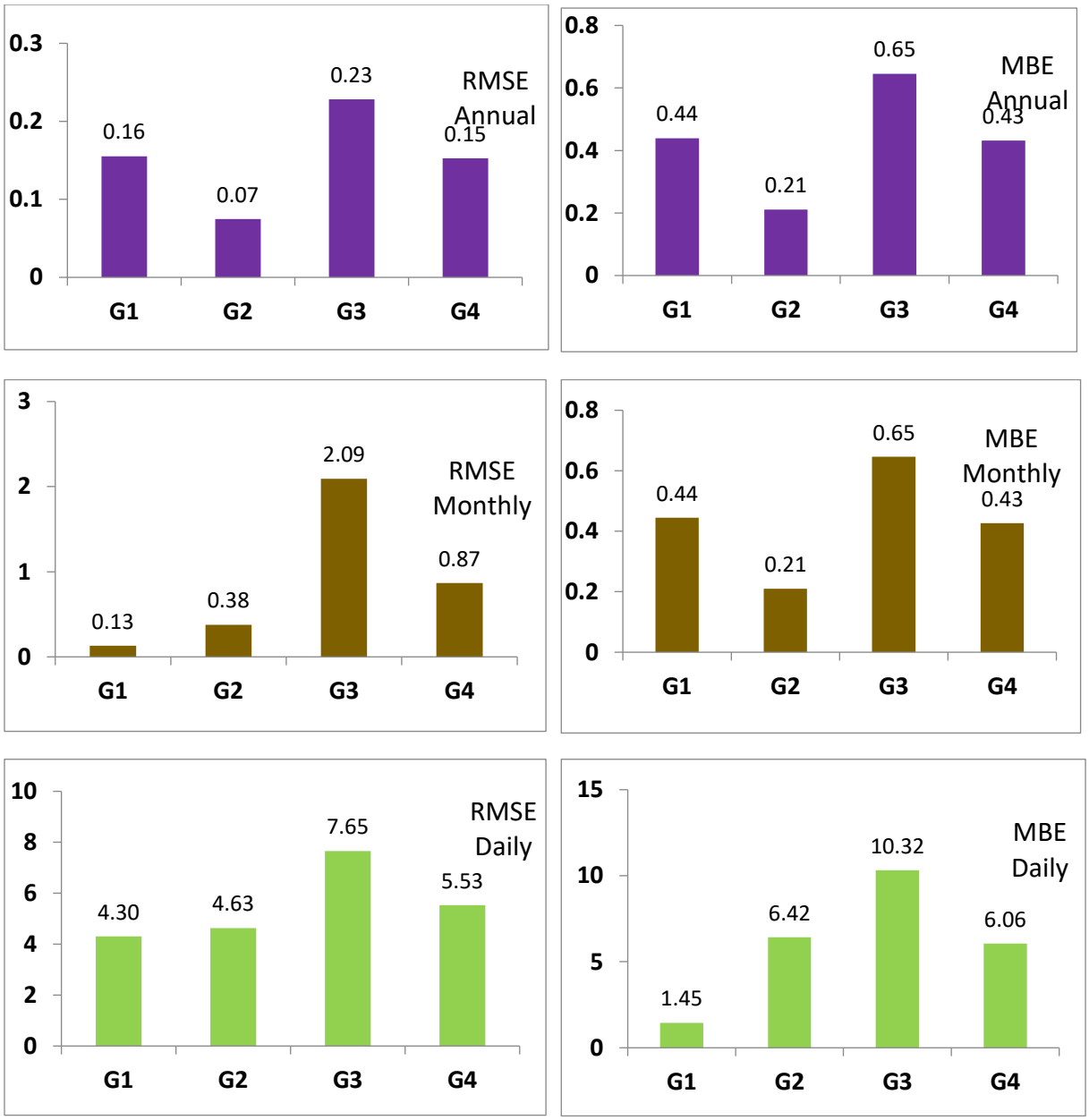

Figure 6. Statistical evaluation (RMSE, MBE) of precipitation using NASA POWER data compared to ground measurements at three-time scales (daily, monthly, and annually).

Annual RMSE values were considerably less than both daily and monthly RMSE values, with annual RMSE values less than 0.23 for all stations, indicating fairly accurate annual precipitation averages. Annually, MBE values were modest (between 0.15 and 0.65), suggesting a fair agreement with actual observations. The NSE values across all stations also indicated a successful performance, reiterating the ability of NASA POWER annual data to represent features associated with the general rainfall climate behavior of the basin. The comparative analysis of the temporal scale indicates that the NASA POWER data begins to perform slightly better with increased aggregation period, with the annual and monthly scales performing more robustly and accurately over the daily scale. This is due to the mitigating effect of temporal aggregation on localized variability and daily fluctuations associated with short-term trends. The high values of R^2 and CC, along with the significant

decrease in RMSE and MBE, suggest that NASA POWER data have the potential to be reliably used as a substitute for ground-based data wherever ground-based monitoring stations are absent in the relatively semi-arid regions and river basins of the Khassa Chai basin. This aligns with what multiple researchers have indicated in similar studies for basins located in the Eastern Mediterranean and northern Iraq **(Tayyeh and Mohammed, 2023)**, where NASA POWER products showed better results than some satellite products, like those from passive microwave sensors, with seasonal precipitation estimations**.**

The results of the statistical analysis of the coefficient of determination (R^2), correlation coefficient (CC), Nash-Sutcliffe efficiency (NSE), root mean square error (RMSE), and mean bias error (MBE) for evaluating the accuracy of satellite-derived precipitation data (NASA POWER) compared to field-measured data in the Khassa Chai River basin at daily, monthly, and annual time scales. The results show that the performance of the satellite data improves with increasing time scale, with R^2 and CC values reaching their highest levels at the monthly (0.9–0.94) and annual (0.81–0.89) scales, reflecting a strong agreement with the observed values, while they decreased at the daily scale to approximately (0.65–0.77) due to the high variability of daily rainfall. The NSE values also showed acceptable performance, ranging between (0.4–0.75), and were positive in most cases, indicating adequate model efficiency, especially at the monthly and annual scales. Conversely, the RMSE values decreased gradually from the daily scale (6–8 mm) to the monthly (1–2 mm) and annual (<1 mm) scales, indicating a decrease in estimation error with increasing time period. The MBE values also showed that the NASA POWER data tended to slightly overestimate daily rainfall (4–8 mm) compared to the measured data, while the annual deviations were very limited (<1 mm). The findings indicate that the satellite data have adequate consistency in representing the temporal distribution of precipitation, especially when looking at the average for the month or the average for the year. Thus, they can be reasonably used for assessments in climate and hydrological studies in the Khassa Chai basin, considering the limited ground-based observation data.

3.2.2 Air Temperature

The assessment of field-measured and NASA POWER (NP) temperature data in the Khassa Chai River basin suggests the temperature data fit well at different timescales as shown in **Figs. 7 and 8**. The values for annual, monthly, and daily were presented with the highest degree of similarity in performance across all stations, while the slight differences were attributed to the unique spatial and climatic reality of the respective region. On the annual timescale, G2 and G3 demonstrated the highest coefficients of determination (R^2 = 0.90), meaning the yearly temperature patterns were most accurately represented, while G1 displayed a slightly lower value (0.88). Correlation coefficients (CC) for all stations were similarly strong (0.94-0.95), suggesting a strong correlation between the system data and field-measured points. Further, the Nash-Sutcliff efficiency (NSE) values were also consistently similar (0.78-0.89), which gave a similarly high level of confidence to conclude the efficiency of annual temperature estimates at each station. The error metrics RMSE were also minimal (0.03–0.11), suggesting the observed and calculated values deviated minimally. Furthermore, MBE results were between -0.08 and 0.31 with an indication that the system overestimated at station G2, while it underestimated at station G1. The variation could be attributed to geographic location effects. G2, situated in the eastern area of the basin, has a flatter terrain and more access to solar radiation, and consequently has a higher surface temperature than the western part of the basin.

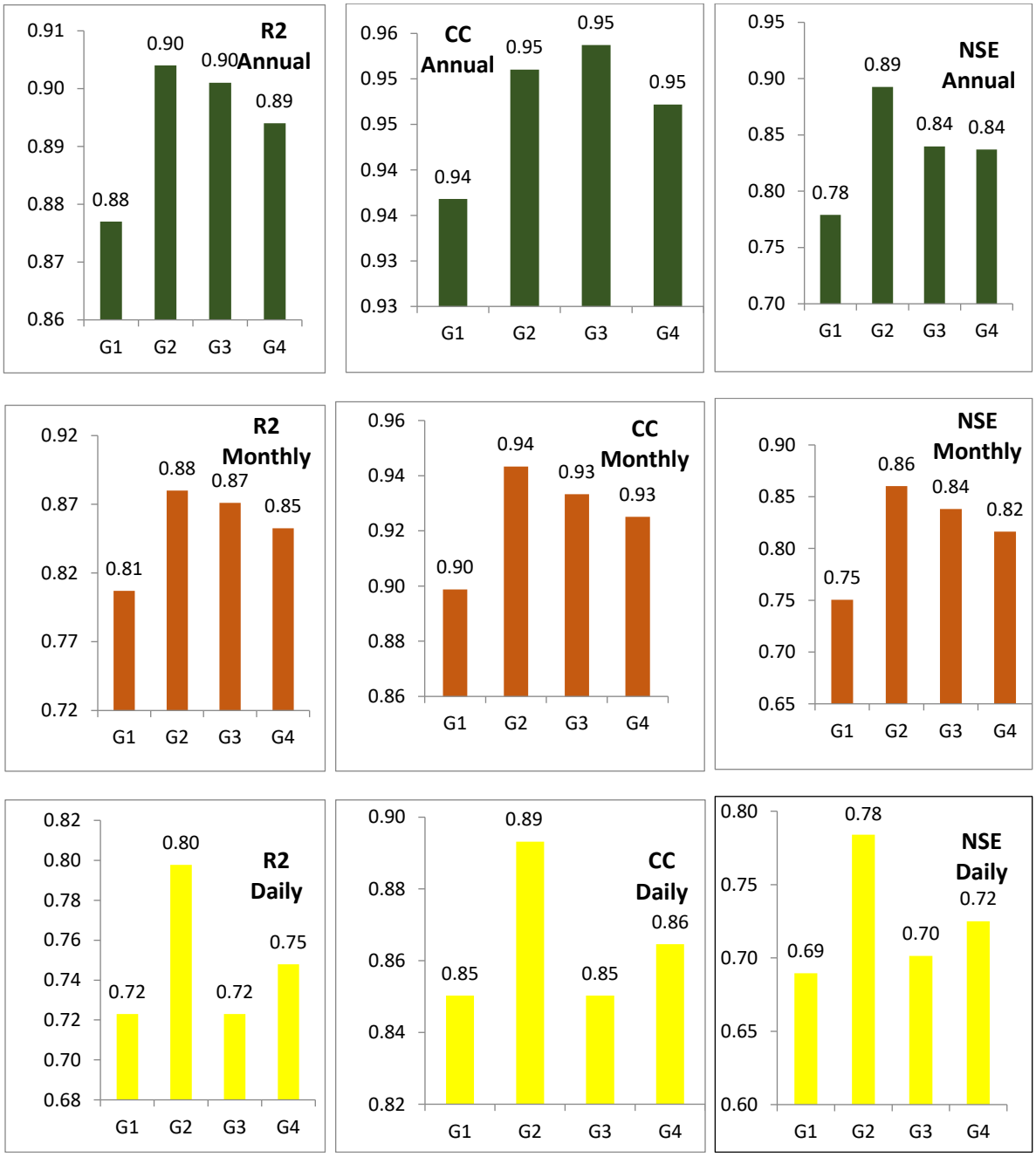

Figure 7. Statistical evaluation (R^2, CC, NSE) of temperature using NASA POWER data compared to ground measurements at three-time scales (daily, monthly, and annually).

At the monthly scale, the data showed very strong Mean Performance by the system with R^2 between 0.81 and 0.88, and CC values between 0.90 and 0.94. The NSE values were also good (0.75-0.86), suggesting that the system is acceptably capturing seasonal variability. Although the RMSE and MBE values showed apparent spatial differences; with G2 reporting the least RMSE (0.12) and G3 the greatest RMSE (0.58) while the MBE ranged from (-0.10 to 1.29), indicating that the system estimates temperatures accurately in the eastern, flatter regions (G2); however, accuracy decreased in the northern, slightly elevated elevations (G3) due to the land cover and topographic variation findings were also affected by not only

elevation and slope; also by the local effects of vegetation cover and humidity. Results showed some expected variation on a daily scale, attributable to the transient nature of temperature fluctuation throughout the day.

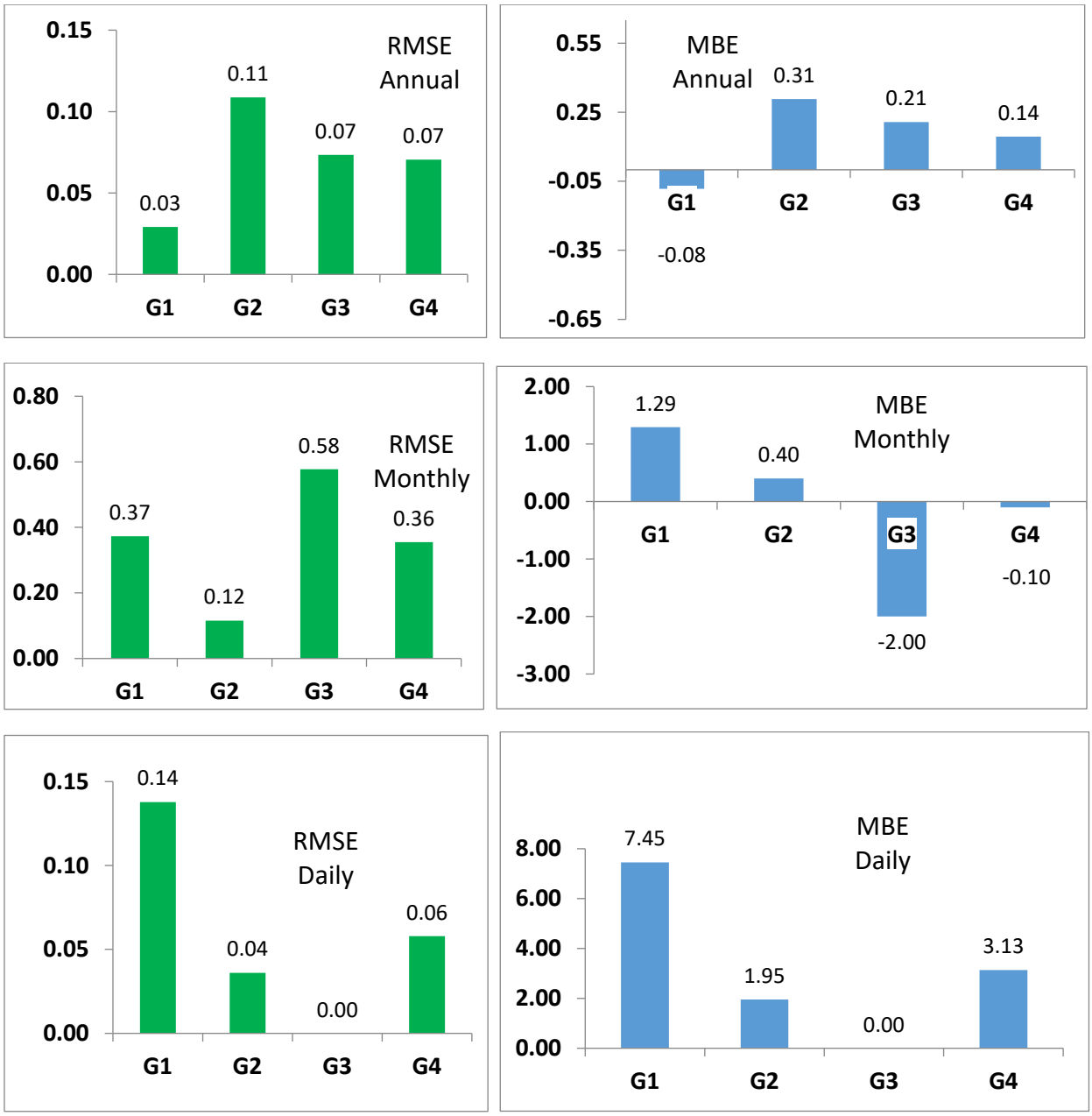

Figure 8. Statistical evaluation (RMSE, MBE) of precipitation using NASA POWER data compared to ground measurements at three-time scales (daily, monthly, and annually).

R^2 values dropped to (0.72–0.80) and NSE to (0.69–0.78), although the correlation (CC = 0.85–0.89) remained strong, indicating the system retained the overall pattern of thermal behaviour, albeit under the large sensitivity to daily fluctuations. The largest values of MBE were associated with G1 (7.45), suggesting a systematic bias to overestimate daily temperatures in the southwestern region, characterized by high evaporation with limited

vegetation and rapid local change. Errors were smaller in G3 (MBE = 0.00) and G4 (3.13), suggesting acceptable agreement in those areas.

The spatial distribution of temperature illustrated in **Fig. 8** shows clear thermal gradients from west to east across the Khassa Chai River basin: the maximum temperature was recorded at station G2 located in the east (22.06–22.17°C), diminishing gradually as moving westward until its lower temperature values at station G4 (21.75–21.85°C). This thermal gradient is strongly related to the general geography of the basin, where eastern parts are generally flatter and at lower elevations, so they receive more solar radiation and are therefore more effective at thermal energy storage. In contrast, western parts have, at least, a relatively higher elevation and steeper slopes down to the river channel and experience the local wind patterns traveling from the west, thereby experiencing cooler temperatures.

The distribution of vegetation cover and surface wetness is still expected to be an important factor to explain, as vegetation density is greater in the western area (near G4), where thermal radiation is reduced, while the eastern area (near G2) has greater with dry soil covers and thus provides greater recorded temperatures. Overall, these analyses confirm cases where the numerical model (NP) demonstrated considerable efficiency in simulating the spatial and temporal distribution of temperatures in the basin, mostly at the annual and monthly levels. Daily estimates should be improved slightly using bias correction methods to reduce differences occurring at stations with more complex topography. These results have shown that model performance is certainly related to the morphometric and topographic characteristics of the basin, while calling into question the need for regionally detailed geographical factors when improving regional climate models.

The results of the (NP) performance evaluation in temperature simulation using Box and Whisker plot, demonstrates the models high efficiency in representing the thermal behavior of the Khassa Chai basin compared to field measurements, with the performance of the model gradually declining between annual to monthly and then daily, reflecting its sensitivity to short-term temporal variability associated with local weather factors, annual coefficient of determination (R^2) ranged from (0.88–0.90) indicating the model explained most variability in measured values, while monthly ranged from (0.84–0.88) and daily from (0.75-0.80). The correlation coefficient (CC) values also showed a very strong correlation between the calculated and measured values (0.94–0.95) at the annual level, and a good correlation monthly (0.91–0.93) and daily (0.86–0.88), indicating that the model can capture the general trend of temperature change in the basin, especially at stations located in the higher-elevation eastern part. The Nash-Sutcliffe efficiency (NSE) ranged from 0.78 to 0.89 on an annual basis, 0.75 to 0.85 every month, and 0.69 to 0.78 daily, indicating that the model is excellent for longer time periods and great when looking at shorter time scales. Likewise, the root mean square error (RMSE) values were low on an annual basis (0.03-0.11), a slight increase for the monthly (as high as 0.58), and daily values (as high as 0.14). This serves to effectively convey model performance in representing both the annual and seasonal range of variability in the temperature, and the increased variability in the daily observations due to local microclimate changes induced by localized factors such as clouds, wind, and humidity. The mean bias error (MBE) estimates near-zero annual bias; bias tends to be about ±2 over the monthly observations and about ±7-degree variability in days. The MBE indicated minor tendencies for the model to over-predict, maximum values on dry sunny days, and predict lower values on low-lying humid days. The noted differences coincide with spatial characteristics of the basin, as the temperature distribution map illustrated in **Fig. 4**, shows an apparent temperature gradient from east to west, with the eastern mountainous

regions (G2) yielding the highest temperature values (22.06-22.17 °C), while grading down toward the west having the lowest temperatures (21.75-21.85 °C) near G4. This variation is attributed to an interaction between topography, vegetation canopy conditions, and surface moisture that may be affecting thermal equilibrium. Overall, these results confirm that the numerical model, NP, demonstrates high efficiency in representing the general thermal behavior of the basin over topographic conditions at the annual and monthly scale, while it could improve the accuracy of the model to represent the daily scale variations by correcting slight bias, particularly on low-lying humid days.

4. CONCLUSIONS

1. The spatial distribution of observation shows a noticeable gradient, where rainfall decreases from 310 mm/year in the cooler northeast hills to about 258 mm/year in the warmer lower southwest; temperature, depending on the transect, varies anywhere from 20.98°C (in the highlands) to 22.84°C (in the lowlands); hence confirming the influence of topography.
2. The accuracy of the NASA POWER data improves proportionally with increasing temporal scale; the agreement between two data sources (two climate data sources) are the greatest at the annual, lower at the monthly, and the least at the daily level; hence discrepancies at shorter time scales can be attributed to short-term (diurnal) variability (e.g., local, land-surface conditions with the short-term climate data comparison) rather than the NASA POWER data, estimation error (RMSE and MBE) significantly decreases from the daily to the monthly and annual analysis, and positive NSE values indicate good data reliability, especially in the monthly/annual analysis.
3. Temperature representation performed well at the monthly and annual level (R^2 and CC > 0.9, NSE ≈ 0.88); however, higher mean daily temperatures are not well represented in drier, highland areas, indicating the need for a local bias correction to improve performance on a daily scale.

NOMENCLATURE

Symbol	Description	Symbol	Description
R^2	Coefficient of Determination, dimensionless	CC	Correction Coefficient, dimensionless
MBE	Mean Bias Error, mm	RMSE	Root Mean Squared Error, mm
NSE	Sutcliffe Efficiency Coefficient, dimensionless		

Credit Authorship Contribution Statement

Alaa Jasim Mohammed: Writing –editing, Validation, Software, Methodology. Basim Sh.Abed: The owner of the project idea – Writing – review & editing. Maysam Th. Al-Hadidi: review.

Declaration of Competing Interest

The authors declare that they have no known competing financial interests or personal relationships that could have appeared to influence the work reported in this paper.

REFERENCES

Abidalla, W.A., and Abed, B.S., 2025. Predicting Future Surface Runoff Delivered to the Euphrates River Using LARSWG and SWAT Models:Sahiliya Valley in the Iraqi Western Desert as a Case Study. *Journal of Engineering*, 31(2), pp. 156-176. https://doi.org/10.31026/j.eng.2025.02.10

Aboelkhair, H., Morsy, M., and El Afandi, G., 2019. Assessment of agroclimatology NASA POWER reanalysis datasets for temperature types and relative humidity at 2 m against ground observations over Egypt. *Advances in Space Research,* 64(1), pp. 129-142. https://doi.org/10.1016/j.asr.2019.03.032

Akkem, Y., Biswas, S.K., and Varanasi, A., 2024. A comprehensive review of synthetic data generation in smart farming by using variational autoencoder and generative adversarial network. *Engineering Applications of Artificial Intelligence*, 131, P. 107881. https://doi.org/10.1016/j.engappai.2024.107881

AL Thamiry, H.A., and Azzubaidi, R.Z., 2020. Survey and discharge measurements of the Iraqi Border crossing rivers. *J. Eng. Sci. Technol*, 15(6), pp. 4288-4302

Ali, A.A., Al-Thamiry, H.A., and Alazawi, S.Q., 2011. Estimation of runoff for Goizha-Dabashan Watershed with aid of remote sensing techniques. *Journal of Engineering*, 17(02), pp. 306-320. https://doi.org/10.31026/j.eng.2011.02.08

Ali, S., Abed, B.S., and Rashid, M., 2023. Generation of IDF equation case study Al-Shuwaija watersheds/(IRAQ-IRAN). *Wasit Journal of Engineering Sciences*, 11(3), pp. 14-26. https://doi.org/10.31185/ejuow.Vol11.Iss3.448

Al-Juhaishi, M.R., Oleiwi, A.S., and Aed, B.S., 2024. Modeling surface runoff in Al-Mohammadi Valley: Influence of climate and soil parameters. *International Journal of Design and Nature and Ecodynamics*, 19(3), pp. 1043-1049. https://.doi.org/10.18280/ijdne.190333

Al-Kahachi, S.A., Al-Tawash, B.S., and Al-Tamimi, O.S., 2022. Distribution and enrichments of abundant and trace elements in Al-Khassa Sub Basin Soil, Kirkuk, Northeastern of Iraq. *Iraqi Journal of Science*, pp. 5338-5352. https://doi.org/10.24996/ijs.2022.63.12.22

Al-Khafaji, M.S., Ibrahim, H.M., and Abdullah, H.S., 2017. Assessment of water clarity within Dokan lake using remote sensing techniques. *Journal of Engineering*, 23(8), pp. 13-28. https://doi.org/10.31026/j.eng.2017.08.02

Al-Kilani, M.R., Rahbeh, M., Al-Bakri, J., Tadesse, T., and Knutson, C., 2021. Evaluation of remotely sensed precipitation estimates from the NASA POWER project for drought detection over Jordan. *Earth Systems and Environment*, 5(3), pp. 561-573. https://doi.org/10.1007/s41748-021-00245-2

Al-Qurnawi, W.S., 2014. Groundwater vulnerability assessment and well head protection zones of Alton Kopry Basin, Kirkuk Governorate Northeast of Iraq. Unpublished Ph. D. Thesis, University of Basrah, Iraq.

Ansari, A., Pranesti, A., Telaumbanua, M., Alam, T., Wulandari, R.A., and Nugroho, B.D.A., 2023. Evaluating the effect of climate change on rice production in Indonesia using multimodelling approach. *Heliyon*, 9(9). https://doi.org/10.1016/j.heliyon.2023.e19639

Bai, W., Wang, G., Huang, F., Sun, Y., Du, Q., Xia, J., Wang, X., Meng, X., Hu, P., Yin, C., and Tan, G., 2025. Review of assimilating spaceborne global navigation satellite system remote sensing data for tropical cyclone forecasting. *Remote Sensing*, 17(1), P. 118. https://doi.org/10.3390/rs17010118

Barron-Lugo, J.A., Lopez-Arevalo, I., Gonzalez-Compean, J.L., Alvarado-Barrientos, M.S., Carretero, J., Sosa-Sosa, V.J., and Montella, R., 2024. A GIS-big data model for improving the coverage and analysis processes of territory observation, and integrating ground-based observations with retrospective meteorological data. *International Journal of Applied Earth Observation and Geoinformation*, 128, P. 103736. https://doi.org/10.1016/j.jag.2024.103736

Baumann, P., Mazzetti, P., Ungar, J., Barbera, R., Barboni, D., Beccati, A., Bigagli, L., Boldrini, E., Bruno, R., Calanducci, A., and Campalani, P., 2016. Big data analytics for earth sciences: the EarthServer approach. *International Journal of Digital Earth*, 9(1), pp. 3-29. https://doi.org/10.1080/17538947.2014.1003106

Bhandari, M., Shrestha, S., and New, J., 2012. Evaluation of weather datasets for building energy simulation. *Energy and Buildings*, 49, pp. 109-118. https://doi.org/10.1016/j.enbuild.2012.01.033

Budamala, V., and Mahindrakar, A.B., 2022. Flexible user interface for machine learning techniques to enhance the complex geospatial hydro-climatic models with future perspective. *Geocarto International*, 37(12), pp. 3469-3488. https://doi.org/10.1080/10106049.2020.1864027

Dawood, A.H., 2024. Flood risk analysis and vulnerability assessment for Erbil area, Doctoral dissertation, Salahaddin University-Erbil.

Faybishenko, B., Versteeg, R., Pastorello, G., Dwivedi, D., Varadharajan, C., and Agarwal, D., 2022. Challenging problems of quality assurance and quality control (QA/QC) of meteorological time series data. *Stochastic Environmental Research and Risk Assessment*, 36(4), pp. 1049-1062. https://doi.org/10.1007/s00477-021-02106-w

Fu, Y., Zhu, Z., Liu, L., Zhan, W., He, T., Shen, H., Zhao, J., Liu, Y., Zhang, H., Liu, Z., and Xue, Y., 2024. Remote sensing time series analysis: A review of data and applications. *Journal of Remote Sensing*, 4, P. 0285. https://doi.org/10.34133/remotesensing.0285

Gu, L., Yin, J., Wang, S., Chen, J., Qin, H., Yan, X., He, S., and Zhao, T., 2023. How well do the multi-satellite and atmospheric reanalysis products perform in hydrological modelling. *Journal of Hydrology*, 617, P. 128920. https://doi.org/10.1016/j.jhydrol.2022.128920

Hazra, A., Maggioni, V., Houser, P., Antil, H., and Noonan, M., 2019. A Monte Carlo-based multi-objective optimization approach to merge different precipitation estimates for land surface modeling. *Journal of Hydrology*, 570, pp. 454-462. https://doi.org/10.1016/j.jhydrol.2018.12.039

Hegyi, B., Stackhouse, P.W., Taylor, P., and Patadia, F., 2024, January. Nasa POWER: providing present and future climate services based on NASA data for the energy, agricultural, and sustainable buildings communities. *In 104th American Meteorological Society (AMS) Annual Meeting*.

Ibrahim, I.A., and Al-Dabbas, M., 2021. Analysis of climate parameters as indicators of climate changes in central and eastern Iraq: Khanaqin climate conditions as a case study. *Iraqi Journal of Science*, pp. 4747-4757. https://doi.org/10.24996/ijs.2021.62.12.13

Jia, A., Liang, S., Wang, D., Mallick, K., Zhou, S., Hu, T., and Xu, S., 2024. Advances in methodology and generation of all-weather land surface temperature products from polar-orbiting and geostationary satellites: A comprehensive review. *IEEE Geoscience and Remote Sensing Magazine*. https://doi.org/10.1109/MGRS.2024.3421268

Jiang, C., Parteli, E.J., Xia, Q., and Shao, Y., 2024. Evaluation of precipitation reanalysis products for regional hydrological modelling in the Yellow River Basin. *Theoretical and Applied Climatology*, 155(4), pp. 2605-2626. https://doi.org/10.1007/s00704-023-04758-w

Kheyruri, Y., Sharafati, A., and Ahmadi Lavin, J., 2024. Performance assessment of NASA POWER temperature product with different time scales in Iran. *Acta Geophysica*, 72(2), pp. 1175-1189. https://doi.org/10.1007/s11600-023-01186-2

Langsdale, M., Verhoelst, T., Povey, A., Schutgens, N., Dowling, T., Lambert, J.C., Compernolle, S., and Kern, S., 2025. The challenges and limitations of validating satellite-derived datasets using independent measurements: lessons learned from essential climate variables. *Surveys in Geophysics*, pp. 1-38. https://doi.org/10.1007/s10712-025-09898-4

Li, H., Zhang, C., Chu, W., and Shen, D., 2023. A process-based deep learning hydrological model for daily rainfall-runoff simulation. *Available at SSRN 4613999*. http://doi.org/10.2139/ssrn.4613999

Li, Z., Jiang, X., and Wang, G., 2024. Numerical models, observing systems, and data assimilation for prediction of ocean mesoscale eddies. *Ocean-Land-Atmosphere Research*, 3, P. 0059. https://doi.org/10.34133/olar.0059

Liu, Z., Shie, C.L., Li, A., and Meyer, D., 2020. NASA global satellite and model data products and services for tropical meteorology and climatology. *Remote Sensing*, 12(17), P. 2821. https://doi.org/10.3390/rs12172821

Mahmood, K.M. and Mohammed-Ali, W.S., 2025. A hydraulic performance model of Khassa Chai River under varying flow conditions. engineering, *Technology & Applied Science Research*, 15(2), pp. 20934-20940. https://doi.org/10.48084/etasr.9675

Mahmoud, M.I., and Kasim, M.N., 2019. Sediment yield problems in Khassa Chai watershed using hydrologic models. *Cihan University-Erbil Scientific Journal*, 3(1), pp. 34-41.

Mankin, K.R., Mehan, S., Green, T.R., and Barnard, D.M., 2025. Review of gridded climate products and their use in hydrological analyses reveals overlaps, gaps, and the need for a more objective approach to selecting model forcing datasets. *Hydrology and Earth System Sciences*, 29(1), pp. 85-108. https://doi.org/10.5194/hess-29-85-2025

Marzouk, O.A., 2021. Assessment of global warming in Al Buraimi, sultanate of Oman based on statistical analysis of NASA POWER data over 39 years, and testing the reliability of NASA POWER against meteorological measurements. *Heliyon*, 7(3). https://doi.org/10.1016/j.heliyon.2021.e06625

Merlone, A., Beges, G., Bottacin, A., Brunet, M., Gilabert, A., Groselj, D., Harper, A., Hechler, P., Ivanov, M., Musacchio, C., and Trewin, B., 2024. Climatological reference stations: Definitions and requirements. *International Journal of Climatology*, 44(5), pp. 1710-1724. https://doi.org/10.1002/joc.8406

Monteiro, L.A., Sentelhas, P.C., and Pedra, G.U., 2018. Assessment of NASA/POWER satellite-based weather system for Brazilian conditions and its impact on sugarcane yield simulation. *International Journal of Climatology*, 38(3), pp. 1571-1581. https://doi.org/10.1002/joc.5282

Mutlu, A., 2025. Comparative evaluation of NASA, ERA5, and observational data for accuracy and reliability. *Theoretical and Applied Climatology*, 156(7), P. 367. https://doi.org/10.1007/s00704-025-05605-w

Nama, A.H., Alwan, I.A., and Pham, Q.B., 2024. Climate change and future challenges to the sustainable management of the Iraqi marshlands. *Environmental Monitoring and Assessment*, 196(1), P. 35. https://doi.org/10.1007/s10661-023-12168-8

Negm, A., Jabro, J., and Provenzano, G., 2017. Assessing the suitability of American National Aeronautics and Space Administration (NASA) agro-climatology archive to predict daily meteorological variables and reference evapotranspiration in Sicily, Italy. *Agricultural and forest meteorology*, 244, pp. 111-121. https://doi.org/10.1016/j.agrformet.2017.05.022

Newman, R., and Noy, I., 2023. The global costs of extreme weather that are attributable to climate change. *Nature Communications*, 14(1), P. 6103. https://doi.org/10.1038/s41467-023-41888-1

Qin, Y., McVicar, T.R., Huang, J., West, S., and Steven, A.D., 2022. On the validity of using ground-based observations to validate geostationary-satellite-derived direct and diffuse surface solar irradiance: Quantifying the spatial mismatch and temporal averaging issues. *Remote Sensing of Environment*, 280, P. 113179. https://doi.org/10.1016/j.rse.2022.113179

Quansah, A.D., Dogbey, F., Asilevi, P.J., Boakye, P., Darkwah, L., Oduro-Kwarteng, S., Sokama-Neuyam, Y.A. and Mensah, P., 2022. Assessment of solar radiation resource from the NASA-POWER reanalysis products for tropical climates in Ghana towards clean energy application. *Scientific reports*, 12(1), P. 10684. https://doi.org/10.1038/s41598-022-14126-9

Rasheed, N.J., Al-Khafaji, M.S., and Alwan, I.A., 2024. Variations of streamflow and sediment yield in the Mosul-Makhool Basin, North Iraq under climate change: a pre-dam construction study. *H2Open Journal*, 7(1), pp. 38-60. https://doi.org/10.2166/h2oj.2023.078

Rodrigues, G.C., and Braga, R.P., 2021. Evaluation of NASA POWER reanalysis products to estimate daily weather variables in a hot summer mediterranean climate. *Agronomy,* 11(6), P. 1207. https://doi.org/10.3390/agronomy11061207

Rouzegari, N., Bolboli Zadeh, M., Jimenez Arellano, C., Afzali Gorooh, V., Nguyen, P., Meng, H., Ferraro, R.R., Kalluri, S., Sorooshian, S. and Hsu, K., 2025. Passive microwave imagers, their applications, and benefits: a review. *Remote Sensing*, 17(9), P. 1654. https://doi.org/10.3390/rs17091654

Saleh, A., Tan, M.L., Yaseen, Z.M., and Zhang, F., 2024. Integrated machine learning models for enhancing tropical rainfall prediction using NASA POWER meteorological data. *Journal of Water and Climate Change*, 15(12), pp. 6022-6042. https://doi.org/10.2166/wcc.2024.719

Schreiner-McGraw, A.P., and Ajami, H., 2021. Combined impacts of uncertainty in precipitation and air temperature on simulated mountain system recharge from an integrated hydrologic model. *Hydrology and Earth System Sciences Discussions*, 2021, pp. 1-30. https://doi.org/10.5194/hess-26-1145-2022

Schuldt, S.J., Nicholson, M.R., Adams, Y.A., and Delorit, J.D., 2021. Weather-related construction delays in a changing climate: a systematic state-of-the-art review. *Sustainability*, 13(5), P. 2861. https://doi.org/10.3390/su13052861

Shao, C., and Nerger, L., 2024. Assimilation of ground-based GNSS data using a local ensemble Kalman filter. Scientific Reports, 14(1), P. 21682. https://doi.org/10.1038/s41598-024-72915-w

Singh, S., Mishra, K., Chavan, R., and Tiwari, H.L., 2023, December. Advancements and challenges in hydrological modeling: a comprehensive review. *In International Conference on Hydraulics, Water Resources and Coastal Engineering,* pp. 423-442. Singapore: Springer Nature Singapore. https://doi.org/10.1007/978-981-97-7474-6_32

Tayyeh, H.K., and Mohammed, R., 2023. Analysis of NASA POWER reanalysis products to predict temperature and precipitation in Euphrates River basin. *Journal of Hydrology*, 619, P. 129327. https://doi.org/10.1016/j.jhydrol.2023.129327

Valipour, M., 2016. How much meteorological information is necessary to achieve reliable accuracy for rainfall estimations?. *Agriculture*, 6(4), P. 53. https://doi.org/10.3390/agriculture6040053

van Leeuwen, C., Sgubin, G., Bois, B., Ollat, N., Swingedouw, D., Zito, S., and Gambetta, G.A., 2024. Climate change impacts and adaptations of wine production. *Nature Reviews Earth & Environment*, 5(4), pp. 258-275. https://doi.org/10.1038/s43017-024-00521-5

Wakweya, R.B., 2023. Challenges and prospects of adopting climate-smart agricultural practices and technologies: Implications for food security. *Journal of Agriculture and Food Research*, 14, P. 100698. https://doi.org/10.1016/j.jafr.2023.100698

Yang, D., Yang, Y., and Xia, J., 2021. Hydrological cycle and water resources in a changing world: A review. *Geography and Sustainability*, 2(2), pp. 115-122. https://doi.org/10.1016/j.geosus.2021.05.003

Zheng, J., and Zhang, S., 2025. Decomposing the total uncertainty in wheat modeling: an analysis of model structure, parameters, weather data inputs, and squared bias contributions. *Agricultural Systems*, 224, P. 104215. https://doi.org/10.1016/j.agsy.2024.104215

تقيم دقة بيانات ناسا باور في تقدير متغيرات الطقس (هطول الامطار ودرجة الحرارة) لمستجمعات مياه نهر خاصة جاي

علاء جاسم محمد[1،*]، باسم شبع عبد[2]، ميسم ثامر مطشر [1،3]

[1]قسم هندسة الموارد المائية، كلية الهندسة، جامعة بغداد، بغداد، العراق

[2]جامعة الهادي، بغداد، العراق

[3] كلية الذكاء الاصطناعي، جامعة بغداد، بغداد، العراق

الخلاصة

تهدف هذه الدراسة التقييم دقة وموثوقية بيانات الاقمار الصناعية من مشروع ناسا باور في التقاط المتغيرات المناخية المهمة، وهي هطول الامطار ودرجة حرارة الهواء، مقارنة بالبيانات التي تم جمعها من محطات الارصاد الجوية الارضية التابعة الى المكز الوطني لبيانات المناخ (NCDC) الموجودة في حوض نهر خاصة جاي. يتميز الحوض بتدرج طوبوغرافي يبدأ من المرتفعات الشمالية الشرقية وينحدر بأتجاه الجنوب الغربي. تشهد اجهزة حوض نهر خاصة جاي مناخا شبه جاف، مع صيف حار وجاف وشتاءا بارد ورطب نسبيا. تم جمع سجلات هطول الامطار ودرجات الحرارة اليومية (2010–2024) من أربع محطات ارصاد جوية، بالإضافة الا سجلات من تسجيل ناسا باور في أقرب نقاط الشبكة لتقييم موثوقية مجموعة البيانات من ناسا باور، استخدمنا العديد من المؤشرات الاحصائية ذات الصلة (معامل، R^2ومعامل الارتباط CC، ومعامل ناش NSE، ومتوسط الخطأ MBE، وجذر متوسط مربع الخطأ RMBSE) على مقاييس زمنية يومية وشهرية وسنوية. اشار تحليل هطول الامطار الى وجود تطابق ممتاز بين بيانات قمر ناسا باور الصناعي والبيانات في الموقع. للمقارنات الشهرية، كانR^2=0.89، CC=0.94 بينما للمقارنات السنوية كان R^2=0.81، .CC=0.88 بشكل عام، تحسن التطابق مع مقاييس زمنية اطول، مما يشير الى قدرة بيانات القمر الصناعي على التقاط اتجاهات هطول الامطار بدقة بمرور الوقت. كما يعزز نطاق قيم NSE من 0.72 الى 0.87 قدرة البيانات على اعادة انتاج تغيرات هطول الامطار بمرور الوقت.

الكلمات المفتاحية: ناسا باور، نهر خاصا جاي، التحقق من بيانات مناخ الاقمار الصناعية، تحليل هطول الامطار ودرجة الحرارة، التوزيع المكاني والزماني.